Zagazig University Medical Journal
www.zumj.journals.ekb.eg

https://doi.org/10.21608/zumj.2021.99578.2369 Volume 30, Issue 1.2, February 2024, Supplement Issue

Manuscript ID ZUMJ-2110-2369 (R1)
DOI 10.21608/ZUMJ.2021.99578.2369

ORIGINAL ARTICLE

Evaluation of Anterior Visual Pathway Lesions Using CT and MRI: A Prospective Descriptive Study

Yassir Edrees Almalki
Radiology Department, College of Medicine, Najran University, Najran, KSA

Corresponding author:
Yassir Edrees Almalki

E-mail:
Almalki.yassir@gmail.com

Submit Date 2021-10-06
Revise Date 2021-10-17
Accept Date 2021-11-09

ABSTRACT

Background: Visual impairment may arise via many diseases. Imaging assessment using computed tomography (CT) and/or magnetic resonance imaging (MRI) can help localize and characterize these kinds of diseases. This study aimed to describe and compare the role of CT and MRI in the evaluation of anterior visual pathway lesions.

Methods: A prospective descriptive study was conducted on 30 patients with symptoms related to the visual pathway (13 females and 17 males; mean age 30.7 ± 8.2 years; range 4-70 years). Considering the anatomical site of lesions, our patients were subdivided into three main groups: optic nerve lesions (n= 9), optic chiasm lesions (n= 17), and lesions involving optic tract and lateral geniculate body (n= 4). The imaging findings of CT and MRI were described and compared.

Results: We found nine patients with optic nerve lesions (five optic nerve gliomas, one optic nerve meningioma, and three lesions infiltrating the optic nerve), 17 patients with optic chiasm lesions (seven pituitary macroadenomas, six craniopharyngiomas, two olfactory groove meningiomas, and two empty sella syndromes), and four patients with lesions involving optic tract and lateral geniculate body (two AVMs, one parasellar meningioma and one acute right thalamic hematoma). MRI is considered an excellent diagnostic modality for providing perfect anatomical details and efficient data concerning the presence, level, and extent of anterior visual pathway lesions, but CT provides greater definition than MRI for bone destruction or erosion as well as for tumoral calcification or acute hemorrhage

Conclusions: CT and MRI are complimentary imaging for evaluating abnormalities of the anterior visual pathway.

Keywords: Anterior visual pathway lesions; CT; MRI

INTRODUCTION

The anterior visual pathway extends from the globes to the lateral geniculate body at the posterolateral aspect of the thalamus. Visual impairment may arise via many diseases as the optic nerve is a fiber tract of the meninges covering the brain; numerous medical processes occurring in the brain and meninges may impact it (1).

The clinical assessment may often indicate the level of visual pathway abnormalities. Different disease processes, however, may lead to a similar visual field problem, such as inflammatory diseases, vascular disorders, and benign and malignant tumors (2). Imaging assessment using computed tomography (CT) and/or magnetic resonance imaging (MRI) can help in localizing and characterizing these kinds of disease; hence the exact cause of visual field defect could be recognized by the radiological assessment (3).

CT is the most appropriate in the assessment of trauma, calcification, and acute hemorrhage. However, MRI is the favorite technique for defining optic nerve pathology, particularly if intracranial extensions occur. Also, it is valuable for detecting and characterizing any abnormalities affecting the seller and reterochiasmal pathway (4). The combined technologies of MRI and CT have provided highly accurate and complementary methods to document visual pathway defects with their underlying neuro-anatomic pathologic substrates (5). The purpose of this research is to describe and compare the roles of CT and MRI in assessing lesions of the anterior visual pathway.

METHODS

Ethics approval:

This prospective observational study was approved by the Institutional Review Board, and informed patient consent was obtained from all participants. The study was done according to The Code of Ethics of the World Medical Association (Declaration of Helsinki) for studies involving humans.

Study population:

Our patients were referred from the Ophthalmology and Neurosurgery departments and the outpatient clinics to CT and MRI units of the Radiology Department. The inclusion criteria included all patients who complained of symptoms related to the visual pathway, hormonal disorders, nasal obstruction, headache, vomiting, anosmia, convulsion, disturbed conscious level, and motor deficit. Exclusion criteria were (i) contraindications to MRI and (ii) pregnant females.

Patient assessment:

All patients were subjected to (i) full history taking, (ii) clinical evaluation included assessment of visual acuity, pupillary testing, fundus examination, visual field testing, and testing of color vision, (iii) renal function tests (creatinine level and GFR), and (iv) radiological examination included CT and MRI. (iv) Follow-up.

CT scanning:

CT scanning was done for all patients in axial and coronal cuts. All CT examinations were performed using 4th generation CT by two scanners (GE sytec Sri and GE Hi-speed. Both axial and coronal cuts were done as follows: (i) Axial view, the patient was examined supine, the beam was parallel to the or bitomeatal line (OML), slice thickness was 2-3 mm, 130 KV, 150m A/sec, and scan time was 1.5 sec. (ii) Coronal view, the patient was examined supine with the neck hyperextend, the beam was perpendicular to the IOML, slice thickness was 2-3 mm, 130 KV, 150m A/sec, and scan time was 1.5 sec. Intravenous (IV) contrast was given to all patients. The dose was 1ml/Kg using nonionic contrast material (Ultravist 370, Bayer Schering Pharma AG, Berlin, Germany).

MR imaging:

MRI studies were performed on all patients using MR Signa contour 0.5-tesla radio-frequency system. All patients were examined supine with the use of an ordinary head coil. Spine echo sequences (SE) were used in all patients. A preliminary T1-WI sagittal image was taken to serve as a locator for future slices. Then, axial images were acquired using multiple pulse sequences, followed by coronal and sagittal images depending on the location of the pathology. Typically, both orbits are examined together. The patient assumes a fixed gaze, straight ahead with the eye open. This allows the patient to concentrate and maintains the eye steady, minimizing motion artefact. T1-WIs were obtained with a repetition time (TR) of 600msec and echo time (TE) of 10 msec. T2-WIs were achieved at a TR of 4000msec and TE of 90 to 102 msec. MRI protocol consistent of T1-WI axial, coronal and sagittal, T2-WI axial, coronal and sagittal, oblique- sagittal parallel to the optic nerve (i.e., 20-30 degrees to the sagittal plane of the head), and contrast-enhanced T1-WIs axial, coronal, and sagittal. All patients were received an IV dosage of Gadolinium DTPA Diethylen Triamine Penta Acetic Acid ranging between 0.1 and 0.2 mmol/Kg.

Follow up:

All patients were followed; 20 had surgical intervention and histological evaluation, and 10 underwent clinical and radiological follow-up.

STATISTICAL ANALYSIS

MedCalc version 11.1 (Mariakerke, Belgium) was used to analyse the data collected. For quantitative data, means and standard deviations were computed. Numbers and percentages were calculated for categorical data and analysed using the Chi-square or Fisher exact test.

RESULTS

Patients:

This study included 30 patients (13 females and 17 males; mean age 30.7 ± 8.2 years; range 4-70 years). The most common age presented among our patients was less than 10 years (n= 8). Diminution of vision was the most common symptom of lesions affecting the anterior visual pathway (n= 30). The patients' data are summarized in Table 1. Considering the anatomical site of lesions, our patients were subdivided into three main groups: optic nerve lesions (n= 9), optic chiasm lesions (n= 17), and lesions involving optic tract and lateral geniculate body (n= 4). The optic chiasm was the most common site affected among our patients (n= 17), the second most common site affected was the optic nerve (n= 9) (Table 2).

Distribution of lesions:

Table 2 shows the distribution of lesions in our study. We founded nine patients with optic nerve lesions (five optic nerve gliomas, one optic nerve meningioma, and three lesions infiltrating the optic nerve), 17 patients with optic chiasm lesions (seven pituitary macro adenomas, six craniopharyngiomas, two olfactory groove meningiomas, and two empty sella syndromes), and four patients with lesions involving optic tract

and lateral geniculate body (two AVMs, one parasellar meningioma, and one acute right thalamic hematoma).

CT and MRI findings:

Table 3 and Table 4 describe the CT and MRI findings of anterior visual pathway lesions, respectively. Comparing both CT and MRI findings in patients of optic nerve glioma, both were equal in detecting the lesion, CT was better in detecting the optic foramen widening. The MRI was better in detecting the full extent of the lesion showing the intracanalicular and intracranial parts of the optic nerve more clearly. Also, MRI revealed other associated brain lesions. Comparing CT and MRI findings in patients of optic nerve meningioma, both were equal in detecting the lesion; however, CT was superior to MRI in detecting the calcification, but MRI was better in delineating the full extent of the lesion. Comparing CT and MRI findings in the patient of recurrent lymphoepithelioma of the right maxillary sinus, both were equal in detecting the lesion. CT was better in detecting the optic foramen widening. At the same time, MRI was better in detecting the full extent of the lesion, showed medial rectus muscle involvement, and differentiated between PNS extension and retained secretion. Comparing CT and MRI findings in patients with nasal squamous cell carcinoma, both were equal in detecting lesion, CT was better in detecting optic foramen widening and bone destruction. At the same time, MRI was better in detecting the full extent of the lesion and intracranial extension and differentiates between PNS extension and retained secretion. Comparing CT and MRI findings in patients of leukemic infiltration of the optic nerve, both were equal in detecting the lesion. CT was better in detecting optic foramen widening. At the same time, MRI was better in detecting the full extent of the lesion and other cerebral associations as meningeal infiltration. Comparing both CT and MRI findings in patients of pituitary macro adenomas, both had the same result in detection of the lesion; however, For the full extent of the lesion and the compression upon optic chiasm, MRI was superior to CT. Also, MRI was better than CT in detecting subacute hematoma within the lesion, which appeared hyper intense at T1 and T2-WIs. Comparing both CT and MRI findings in patients of craniopharyngiomas, both were equal in the detection of the lesion, CT was better in the detection of calcification and cyst formation; however, MRI was better in the detection of the full extent of the lesion and the compression upon optic chiasm. CT was better than MRI in the detection of the hemorrhage within the lesion. Comparing CT and MRI findings in patients of olfactory groove meningiomas, both were equal in detecting the lesion, CT was better in the detection of calcification. At the same time, MRI was better in detecting the full extent of lesion and compression upon optic chiasm. Comparing CT and MRI findings in patients of AVM, both had the same result in detection of the lesion; however, for the full extent of the lesion and the compression upon optic tract and lateral geniculate body, MRI was superior to CT. Also, MRA enables the detection of the feeding arteries. Comparing both CT and MRI findings in patients of parasellar meningioma, both were equal in detecting lesion; however, MRI was better in the detection of full extent of lesion, showing the enhanced dural tail and signal void carotid artery. Comparing CT and MRI findings in patients of acute right thalamic hematoma revealed that CT was better than MRI in detecting lesions.

Representative cases of our study are illustrated in Figs. 1-4.

Table 1. Patients' data

	Value
Age (years), Mean ± SD (range)	30.7 ± 8.2 (4-70)
Sex	
Male	17 (56.7)
Female	13 (43.4)
Symptoms	
Diminution of vision	30 (100)
Proptosis	5 (16.7)
Headache	17 (56.7)
Symptoms of hormonal disorders	5 (16.7)
Vomiting	4 (13)
Anosmia	3 (10)
Disturbed conscious	3 (10)
Motor deficit	4 (13)
Visual defect	3 (10)
Convulsion	1 (3.3)

Unless otherwise indicated, date represent the number of patients and percentage in parenthesis
SD= standard deviation

Table 2. Distribution of lesions

Lesions	Value
A. Optic nerve lesions	9 (30)
a. Lesions originating from optic nerve or its sheath	6 (20)
1. Optic nerve gliomas	5 (16.7)
2. Optic nerve sheath meningioma	1 (3.3)
b. Lesions infiltrating optic nerve	3 (10)
1. Recurrent lymphoepithelioma at maxillary sinus	1 (3.3)
2. Nasal squamous cell carcinoma	1 (3.3)
3. Leukemia infiltration of optic nerve	1 (3.3)
B. Optic chiasma lesions	17 (57)
1. Pituitary macroadenoma	7 (23.3)
2. Craniopharyngioma	6 (20)
3. Olfactory groove meningioma	2 (6.7)
4. Empty sella syndrome	2 (6.7)
C. Lesions involving optic tract and Lateral geniculate body	4 (13)
1. AVM	2 (6.7)
2. Parasellar meningioma	1 (3.3)
3. Acute thalamic hematoma	1 (3.3)

Date represent the number of patients and percentage in parenthesis
AVM= arteriovenous malformation

Table 3. CT findings of anterior visual pathway lesions

Lesions	CT findings
Optic nerve gliomas	Marked enlargement, kinking and buckling of the affected optic nerve. Widening of optic foramen was detected in 4 cases. Contrast administration revealed mild homogeneous enhancement in 4 cases with no contrast enhancement in one case
Optic nerve sheath meningioma	A well-defined dense tubular mass surrounds and parallels the left optic nerve with homogeneous and well-defined contrast enhancement. Granular calcification was seen within the mass. The enhanced axial scans showed hypodensity (optic nerve) in the center of the enhanced mass giving the appearance of tram-track sign.
Recurrent lymphoepithelioma at maxillary sinus	An ill-defined isodense soft tissue mass is seen at the anatomical site of the right maxillary sinus with both infratemporal and intraorbital extension infiltrating the intraorbital part of the right optic nerve with a widening of the right optic foramen. Also, there was losing of aeration seen involving right ethmoidal air cells and sphenoid sinus. The lesion displayed mild homogeneous post-contrast enhancement
Nasal squamous cell carcinoma	Large ill-defined isodense mass at the right nasal cavity extends to the right orbit and infiltrates the right optic nerve with widening the right optic foramen. In addition, there was a loss of aeration at the right maxillary and ethmoidal air cells with bone destruction involving the orbital floor and lamina papyracea. The lesion displayed heterogeneous post-contrast enhancement
Leukemia infiltration of optic nerve	A soft tissue density lesion involving the intraconal part of the left optic nerve with a widening of left optic foramen. The lesion displayed isodensity with mild post-contrast enhancement
Pituitary macroadenoma	A well-defined isodense sellar lesion with suprasellar extension. Four cases showed homogeneous post-contrast enhancement; the other 3 cases showed heterogeneous post-contrast enhancement. Cystic changes were seen in 3 cases. Two cases showed compression upon the third ventricle leading to dilatation of both lateral ventricles. One case had bilateral parasellar extension
Craniopharyngioma	Sellar and suprasellar well defined mixed attenuation lesions with a solid and cystic component. Five cases showed hydrocephalic changes. Calcification was seen in 2 cases. A haemorrhage was seen in one case (acute). All cases showed heterogeneous post-contrast enhancement except one case showed no enhancement
Olfactory groove	Isodense to hyperdense bifrontal space-occupying lesion. After contrast administration, one

meningioma	case showed homogeneous enhancement, and the other case showed heterogeneous enhancement. The two cases showed mild to moderate perifocal edema. One case showed a mass effect in the form of splaying frontal horns of both lateral ventricles. Calcification was seen in two cases
Empty sella syndrome	Ballooning of sella turcica with CSF density like filling it with no contrast enhancement
AVM	Variable sized serpiginous shaped isodense lesions with areas of calcification. The lesion showed effacement upon related lateral ventricle with heterogeneous post-contrast enhancement
Parasellar meningioma	Hyperdense lesion is seen at right parasellar space with intense homogeneous post-contrast enhancement
Acute thalamic hematoma	A well-defined hyperdense area of fresh blood density at the right thalamic region

AVM= arteriovenous malformation

Table 4. MRI findings of anterior visual pathway lesions

Lesions	MRI findings
Optic nerve gliomas	Enlarged, thickened optic nerve with kinking and buckling. The lesion displayed isointense signal at T1-WI in all cases, hyperintense signal at T2-WI in 4 cases and isointense signal at T2-WI in one case. After contrast administration, mild to moderate homogeneous enhancement was seen in 4 cases with no enhancement in one case. Widening of optic foramen was seen in one case. In the case of bilateral optic nerve glioma with neurofibromatosis type I, MRI of the brain showed areas of abnormal signal intensity displayed hypointense signal at T1-WI and hyperintense signal at T2-WI with no post contrast enhancement denoting heterotopia
Optic nerve sheath meningioma	A normal-sized left optic nerve, concentrically surrounded by a homogeneously enhancing mass extending from the globe to the optic foramen. The tumor retains an isointense appearance to the optic nerve and brain tissue on both T1 and T2-WIs.
Recurrent lymphoepithelioma at maxillary sinus	The full extent of the lesion was demonstrated, and the involved right optic nerve appeared more thickened and enlarged. The lesion displayed isointense signal at both T1 and T2-WIs with mild homogeneous post-contrast enhancement. The right medial rectus muscle was also involved as it showed abnormal thickening (comparing to the opposite side). At T2-WI, the ethmoidal air cells and sphenoid sinus showed high signal intensity denoting retained secretion
Nasal squamous cell carcinoma	The full extent of the lesion was demonstrated with infiltration of the right optic nerve, ethmoidal air cells and intracranially. The lesion displayed mixed intensity at T1 and T2-WIs with heterogeneous post-contrast enhancement sparing the cystic changes. At T2-WI, the right maxillary sinus showed high signal intensity denoting retained secretion.
Leukemia infiltration of optic nerve	More extension of the lesion involving the intraconal and intracanalicular parts of the left optic nerve was demonstrated. The lesion displayed hypointense signal at both T1 and T2-WIs with intense homogeneous post-contrast enhancement, associated with diffuse meningeal infiltration in the form of enhanced thickened meningeal lining seen at post-contrast coronal MRI.
Pituitary macroadenoma	A well-defined lobulated sellar Space occupying lesions. At T1-WI, 3 cases were isointense, one case was hyperintense, and the other 3 cases showed areas of cystic changes. At T2-WI, the lesions displayed an isointense signal in 3 cases and a hyperintense signal in one case; the other 3 cases showed heterogeneous signals due to areas of cystic changes. All lesions had suprasellar extension compressing upon optic chiasm. Four cases showed homogeneous post-contrast enhancement; the other 3 cases showed heterogeneous post-contrast enhancement. Two cases showed hemorrhage (subacute phase) appeared hyperintense at T1 and T2-WIs. Two cases showed compression upon the third ventricle leading to dilatation of both lateral ventricles. One case had bilateral parasellar extension
Craniopharyngioma	Sellar and suprasellar well-defined space-occupying lesion of mixed-signal intensity at T1 and T2-WIs. Five cases showed hydrocephalic changes. Signal void calcifications were seen in one case. All cases showed heterogeneous post-contrast enhancement, except one case showed no enhancement.
Olfactory groove meningioma	Bifrontal space-occupying lesion, isointense at T1-WI, hyperintense at T2-WIs with intense homogeneous post contrast enhancement. The lesions were seen infiltrating both ethmoidal air cells. Compression upon optic chiasm was better seen at coronal planes. Signal void calcification was detected in one case.
Empty sella syndrome	Ballooning of sella turcica with abnormal signal intensity filling it, low signal intensity at

	T1-WIs and high signal intensity at T2-WIs with no contrast enhancement.
AVM	Variable sized, serpiginous shaped, mixed-signal intensity lesions at T1 and T2-WIs with effacement upon related lateral ventricle. Heterogeneous post-contrast enhancement was seen. MRA revealed large vascular lesions with dilated feeding arteries and draining veins.
Parasellar meningioma	Right parasellar space-occupying lesion, isointense at T1-WI, and hyperintense at T2-WI with intense homogeneous post-contrast enhancement and characteristically enhanced dural tail. The lesion was encasing the cavernous sinus as well as the siphon of the carotid artery; however, a normal signal void of the artery was seen.
Acute thalamic hematoma	Abnormal signal intensity lesion at right thalamic region and internal capsule. The lesion displayed isointense signal intensity at T1-WI and mixed-signal intensity at T2-WI

AVM= arteriovenous malformation

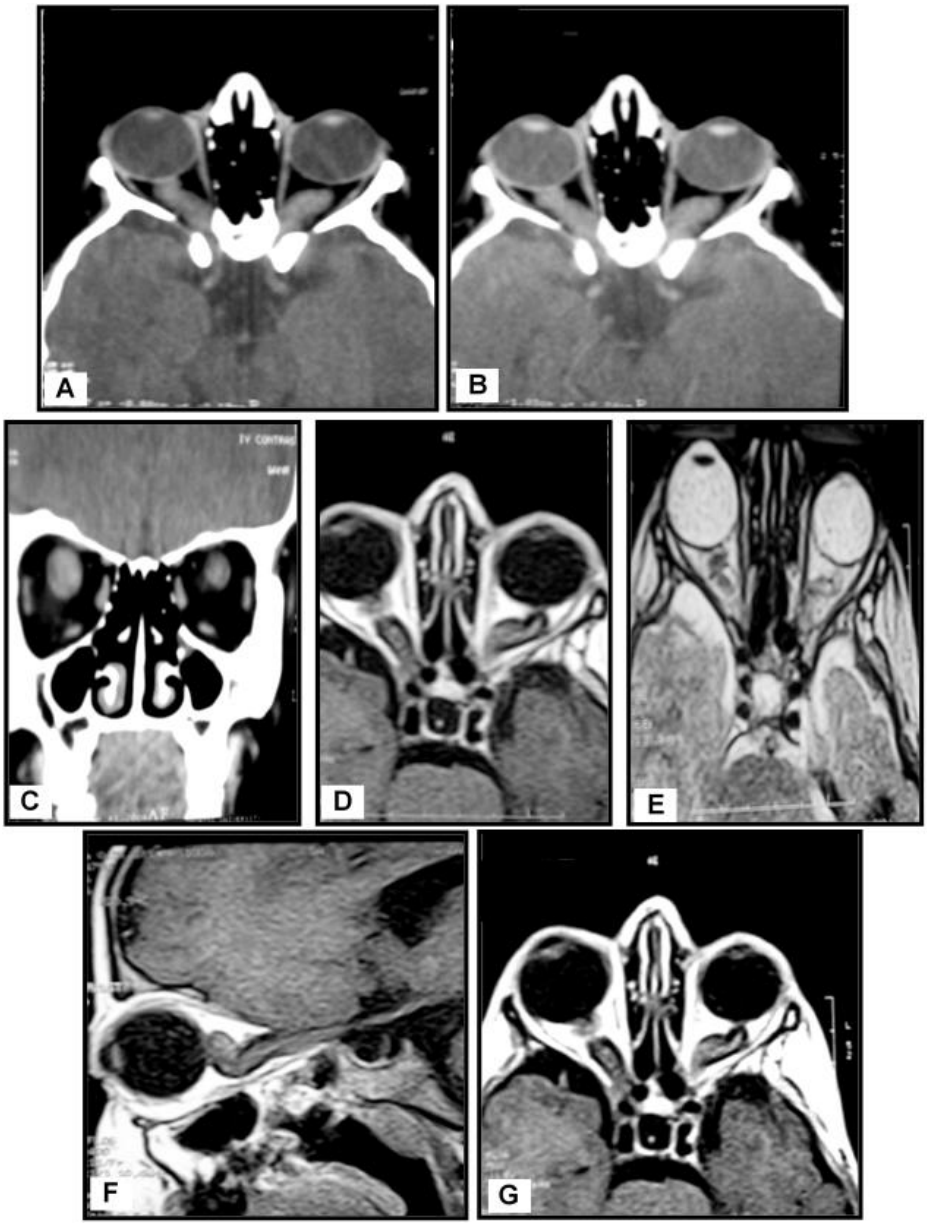

Figure 1. Bilateral optic nerve glioma. A 14-year-old female patient presented with diminution of vision and Proptosis at both eyes. CT Examination: (A) Axial Cuts show marked enlargement, kinking and buckling of both optic nerves with a widening of both optic foramina. (B) and (C) Post-contrast axial and coronal cuts of the same patient show mild homogeneous enhancement. MRI Examination: (D) Axial T1-WI of the same patient shows both enlarged optic nerves displaying an isointense signal. (E) Axial T2-WI of the same patient shows an isointense signal of the lesion. (F) Post-contrast sagittal oblique T1-WI of the same patient reveals enlargement, kinking and buckling of the right optic nerve with mild enhancement. (G) Post-contrast axial T1-WI of the same patient shows mild enhancement.

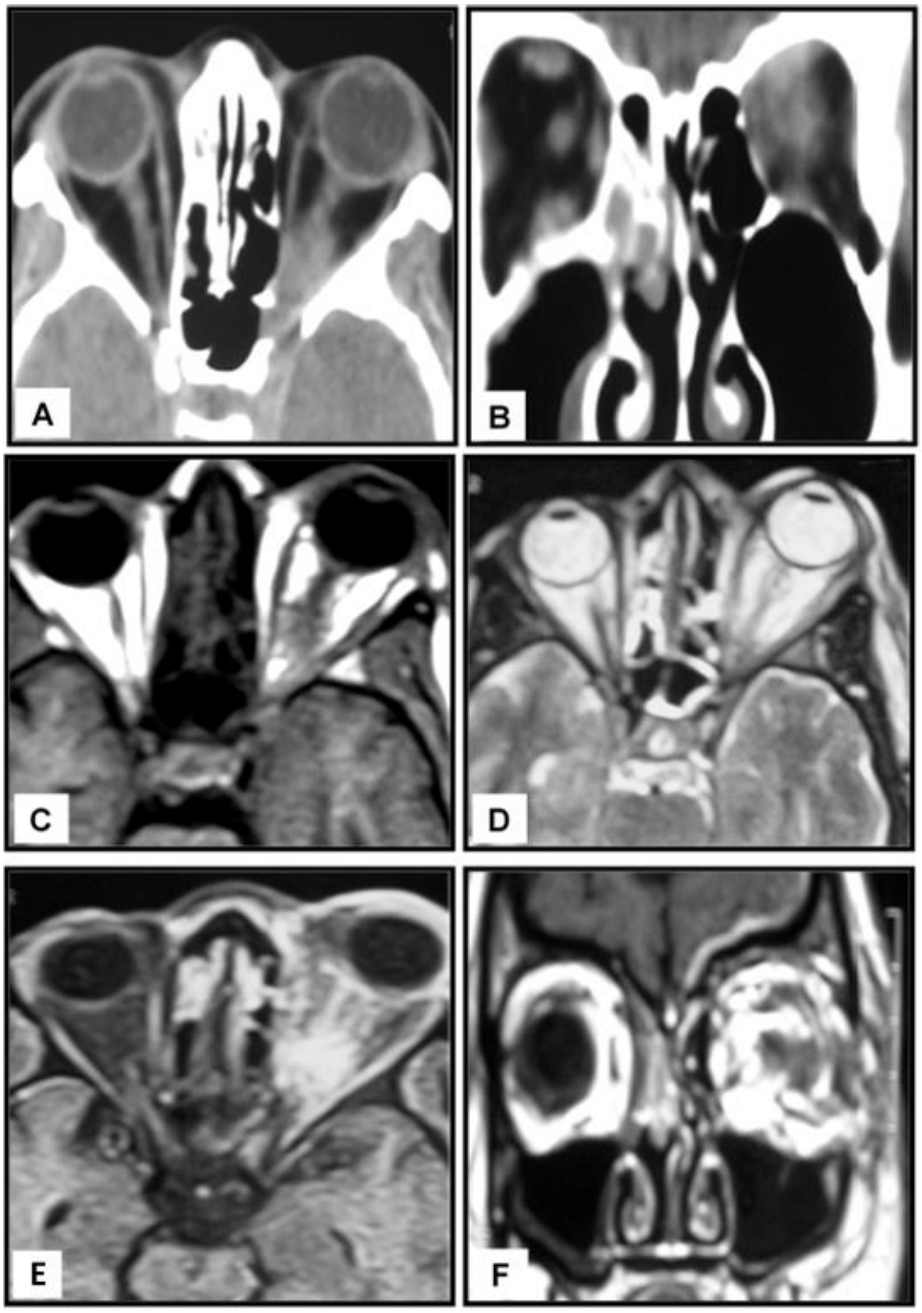

Figure 2. Leukemic infiltration of the left optic nerve. A 36-year-old female patient has a history of acute lymphoplastic leukemia (ALL), complaining of gradual diminution of vision and proptosis at the left eye. CT Examination: (A) and (B) Post-contrast axial and coronal cuts show a soft tissue density lesion involving the intraconal part of the left optic nerve with a widening of left optic foramen. MRI Examination: (C) Axial T1-WI of the same patient shows the lesion displaying hypointense signal and involving the intraconal and intracanalicular parts of the left optic nerve. (D) Axial T2-WI of the same patient shows a hypointense signal of the lesion. (E) and (F) Post-contrast axial and coronal T1-WI of the same patient reveal intense homogeneous post-contrast enhancement of the lesion with diffuse meningeal infiltration in the form of the enhanced thickened meningeal lining.

Figure 3. Pituitary macroadenoma. A 47-year-old female patient presented with diminution of vision and headache. CT Examination: (A) Axial cuts show a well-defined sellar lesion with suprasellar extension compressing upon the third ventricle with dilatation of frontal horns of both lateral ventricles. The lesion is isodense with a small cystic area seen inside. (B) and (C) Post-contrast axial and coronal cuts of the same patient show intense homogeneous enhancement of lesion sparing cystic area. MRI examination: (D) an (E) Axial and coronal T1-W1 of the same patient shows a well-defined isointense sellar Space occupying lesion with suprasellar extension compressing upon optic chiasm. The lesion showed a small area of hyperintensity. (F) Coronal T2-W1 of the same patient shows a heterogeneous intensity of the lesion. The small hyperintense area is seen at T1WI also appeared hyperintense at T2WI, denoting subacute hematoma. (G), (H), and (I) Post-contrast axial, coronal and sagittal T1-W1 of the same patient show a heterogeneous enhancement of the lesion.

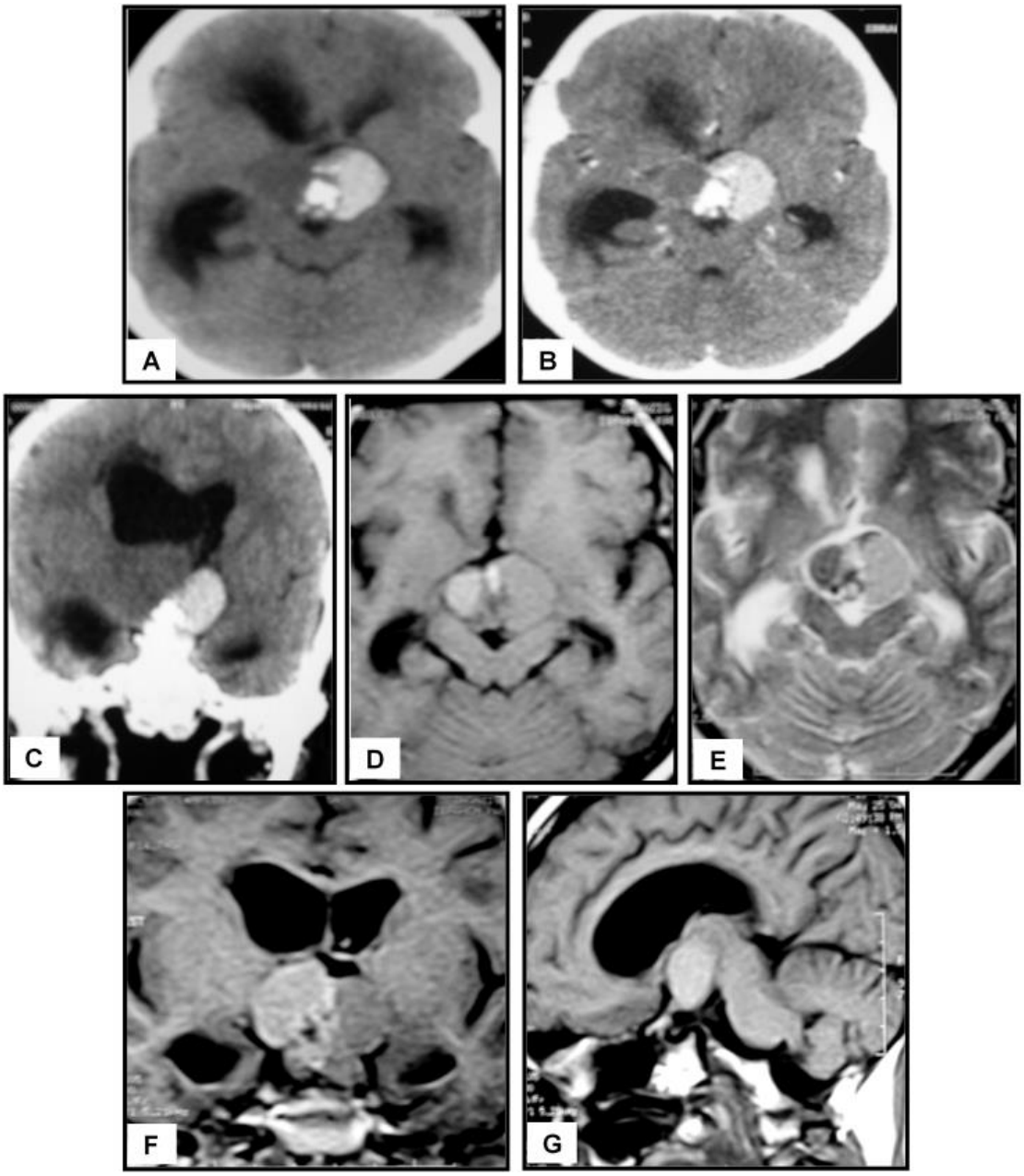

Figure 4. Craniopharyngioma. A 13-year-old male patient presented with diminution of vision and headache. CT Examination: (A) Axial cuts show suprasellar, well-defined mixed attenuation lesion with solid and cystic components. Areas of fresh blood and dense calcification are seen within the lesion. The lesion compresses upon the third ventricle with dilatation of both lateral ventricles. (B) and (C) Post-contrast axial and coronal cuts of the same patient show no enhancement of the lesion. MRI Examination: (D) Axial T1WI of the same patient shows suprasellar well-defined space-occupying lesion of mixed-signal intensity. (E) Axial T2-WI of the same patient shows the mixed-signal intensity of the lesion. (F) and (G) Post-contrast coronal and sagittal T1-WI of the same patient shows no enhancement of the lesion. The lesion is seen compressing upon optic chiasm and third ventricle with dilatation of both lateral ventricles.

DISCUSSION

The current study included 9 patients with optic nerve lesions, 5 patients had optic nerve glioma. The CT findings of optic nerve gliomas are agreeing with Hollander et al. (6), who reported that on CT scans, the affected optic nerve is enlarged in a fusiform shape with kinking and buckling with variable enhancement after contrast administration. The MRI findings agree with Orlando et al. (7), who reported that optic nerve gliomas show decreased or intermediate signal intensity on T1-WI and high signal intensity on T2-WI with variable contrast enhancement.

Holman et al. (8) compared MRI of the optic nerves and chiasm with CT in four patients with biopsy-confirmed or suspected optic gliomas. They found that: both techniques effectively visualized orbital abnormalities, normal optic

nerves and gliomatous had comparable spin-echo MRI features, MRI was better than contrast-enhanced CT in identifying intracranial optic nerves, chiasm, and optic tracts, but CT better outlined orbital anatomic and spatial relationships. These results are similar to our results. Miller (9) reported that benign glioma is the most common primary tumour of the optic nerve. Typically, this low-grade astrocytoma can be followed without intervention. Often, but not permanently, the diagnosis may be established using the findings of a comprehensive examination in conjunction with imaging modalities, especially CT and MR imaging. This agrees with our results. Also agree with the results of Melissa and Meldrum (10), who stated that biopsy of the optic nerve glioma is not often required because of the characteristic appearance of these lesions on radiographic studies. Also, Jacobson (11) mentioned that diagnostic biopsy is not required in most cases of childhood gliomas.

Our study included one case of optic nerve sheath meningioma. The CT findings are consistent with Saeed et al. (12), who reported that imaging revealed segmental or widespread thickening of the optic nerve sheath or globular growth. Calcification occurred in 31% of cases and was accompanied by slower tumour growth. According to Orlando et al. (13), in both T1 and T2-weighted MR images, optic nerve sheath meningioma is isointense to the optic nerve. This agrees with our results. The optic nerve tram-track sign is most commonly associated with optic nerve sheath meningiomas (14). This similar to our results. Our results revealed that both CT and MRI were equal in detecting optic nerve meningioma; however, CT was superior to MRI in detecting the calcification, but MRI was better in delineating the full extent of the lesion. This agrees with Mafee et al. (15).

Optic nerve infiltrative lesions are rare. CT and MRI showed swelling of the optic nerves, a finding consistent with inflammatory or malignant disease (16). This agrees with our result, which included 3 cases with optic nerve infiltration in which the optic nerve appeared enlarged and thickened.

Lundin et al. (17) concluded that MR was superior to CT in macroadenoma. The superiority of MR was particularly evident in terms of cavernous sinus invasion and the relationship of the tumour to the carotid arteries and optic chiasm. Also, Webb et al. (18) stated that in macroadenomas, both CT and MRI are equally diagnostic, but magnetic resonance offers more information on pituitary morphology and neighbouring structures. This agrees with our results.

Kanchan et al. (19) stated that craniopharyngiomas are classically seen on CT scans as cystic suprasellar mass with some solid constituents. A heterogeneous suprasellar mass with varied appearances is seen on MR imaging, particularly on T1-weighted images. The most frequent pattern is a cyst with low signal intensity on T1-weighted images and high signal intensity on T2-weighted imaging. These agree with the current study. Anderson et al. (20) noted that calcification is prevalent, particularly in paediatric tumours, and is best seen with CT. This agrees with our results as two cases showed calcification best seen by CT. Comparing CT and MRI findings in cases of craniopharyngiomas revealed that; both were equal in detecting the lesion, CT was better in detecting calcification and cyst formation; however, MRI was better in the detection of calcification and cyst formation detection of full extent of lesion and compression upon optic chiasm. These results were similar to Freeman et al. (21).

The findings of CT and MRI in our olfactory groove meningioma cases are similar to Obied and Al-Mefty (22), who found that olfactory groove meningioma invading the underlying bone with a high rate of late recurrence; the sites of these recurrences were the cranial base and adjacent paranasal sinuses. Our cases of meningioma revealed a bifrontal lesion with surrounded brain oedema, which is similar to Nakano et al. (23).

When CT and MRI findings were compared, our results were substantially identical to those of Pott et al. (24), who show that MRI is better than CT in identifying and distinguishing AVM. Its strength is in its ability to identify aberrant vessels even in the presence of new or older haematoma, as well as in the exact information it provides about the AVM's size and location.

In our study, there was one case of parasellar meningioma. The CT findings are to the Mafee et al. (25), who stated that parasellar meningiomas have slight to moderate high attenuation on plain CT scans compared to brain meningiomas. Our MRI findings are relatively similar to Elster et al. (26), who stated that most meningiomas are isointense to the brain on T1 and T2-WIs with intense post-contrast enhancement, with a characteristic broad base of attachment against the dural surface. Our study revealed that MRI was better in detecting the full extent of the lesion, showing the relation of the mass to the surrounding structures as the carotid artery,

cavernous sinus, optic tract and lateral geniculate body. This is similar to Young et al. (27).

Our study encounters one case of acute thalamic hematoma; the CT findings are similar to the Kasuya et al. (28).

Our study had some limitations. First, small sample size and second, all examinations were performed on 0.5 Tesla MRI.

Conclusion:

We can conclude that CT and MRI complement each other in evaluating anterior visual pathway lesions. MRI is considered an excellent diagnostic modality for providing perfect anatomical details and efficient data concerning the presence, level and extent of anterior visual pathway lesions. CT provides a greater definition than MRI for bone destruction or erosion, tumor calcification, or acute hemorrhage. However, several factors could affect the choice of technique in imaging anterior visual tract lesions. First, the clinician should be able to limit his focus on the possible differential diagnosis and anatomical sites of lesions by thorough history taking and physical examination; then, it must be decided which of the available technologies will be more precise in detecting suspected lesions.

Declaration of interest:

The author declares no relevant conflicts of interest and no relationships with any companies whose products or services may be related to the article's subject matter.

Funding information:

The authors state that this work has not received any funding.

REFERENCES:

1. **Kang JS, Zheng Z, Choi MJ, Lee SH, Kim DY, Cho SB.** The effect of CD34+cell-containing autologous platelet-rich plasma injection on pattern hair loss: A preliminary study. J Eur Acad Dermatol Venereol. 2014;28:72–9……. Smith MM, and Strottmann JM. Imaging of the optic nerve and visual pathways. Semin Ultrasound CT MR. 2001; 22(6):473-7.
2. **Weber AL, Klufan R, and Pless M**. Imaging evaluation of the optic nerve and visual pathway. Neuroimaging Clin North Am 1996; 6:143-77.
3. **Thompson CR and Lessel S**. Anterior visual pathway gliomas. Int Ophthalmol Clin 1997; 37: 261-79.
4. **Bose S**. Neuroimaging in neuroophthalmology. Neurosurg Focus. 2007; 23(5):E9.
5. **Alvord EC, Lofton S**. Gliomas of the optic nerve or chiasm: outcome by patients' age, tumor site, and treatment. Journal of neurosurgery. 1988; 68(1):85-98.
6. **Hollander M, FitzPatrick M, O'connor SG, Flanders AE, Tartaglino LM**. Optic gliomas, RCNA. 1999;37(1): 59-71.
7. **Orlando O, Sydney S, Jeffrey M, and David K**. Radiologic-pathologic correlation: Meningioma of the optic nerve sheath. AJNR. 1996:901-6.
8. **Holman RE, Grimson BS, Drayer BP, Buckley EG, Brennan MW**. Magnetic resonance imaging of optic gliomas. Am J Ophthalmol. 1985; 100(4):596-601.
9. **Miller NR**.: Primary tumors of the optic nerve and its sheath. Cambridge Ophthalmological Symposium. 2004; 18 (11): 1026-37.
10. **Melissa L and Meldrum MD**. Pediatric orbital tumor. Ophthalmology Clinic of North America. 1999; 12(2): 279-91.
11. **Jacobson DM**. Glioma of anterior visual pathways. Neurosurg Clin N Am. 1999; 10(4): 683-98.
12. **Saeed P, Rootman J, Nugent RA, White VA, Mackenzie IR, Koornneef L**. Optic nerve sheath meningiomas. Ophthalmology. 2003; 110(10):2019-130.
13. **Orlando O, Sydney S, Jeffrey M, David K**. Radiologic-pathologic correlation: Meningioma of the optic nerve sheath. AJNR. 1996; 17:901-6.
14. **Uday S, and Kanamalla.** The Optic Nerve Tram-Track Sign. Radiology. 2003; 227:718-719.
15. **Mafee MF, Goodwin J, Dorodi S**. Optic nerve sheath meningioma. RCNA. 1999; 37(1): 37-58.
16. **Abdollah A, Tampieri D, Kirkham TH, Melanson D**. Computed tomography and magnetic resonance imaging of an infiltrative lesion of the anterior visual pathways. Can Assoc Radiol J. 1991; 42(1):60-3.
17. **Lundin P, Bergstrom K, Thuomas KA, Lundberg PO, Muhr C**. Comparison of MR imaging and CT in pituitary macroadenomas. Acta Radiol. 1991; 32(3):189-96.
18. **Webb SM, Ruscalleda J, Schwarzstein D, Calaf-Alsina J, Rovira A, Matos G, et al**. Computerized tomography versus magnetic resonance imaging: a comparative study in hypothalamic-pituitary and parasellar pathology. Clinical endocrinology. 1992; 36(5):459-65.
19. **Kanchan Gupta A, Matthew J, Kuhna, Douglas W, Shevlina, Lyle E**. Metastatic Craniopharyngioma. American Journal of Neuroradiology. 1999; 20:1059-60.

20. **Anderson JR, Antoun N, Burnet N, Chatterjee K, Edwards O, Pickard JD, Set al**. Neurology of the pituitary gland. J Neurol Neurosurg Psychiatry. 1999; 66(6):703-21.
21. **Freeman MP, Kessler RM, Allen JH, Price A.C**. Craniopharyngioma: CT and MR imaging in nine cases. J Comput Assist Tomogr. 1987; 11(5):810-14.
22. **Obeid F and Al-Mefty O**. Recurrence of olfactory groove meningiomas. Neurosurgery. 2003; 53(3): 534-42.
23. **Nakano T, Asano K, Miura H, Itoh S, Suzuki S**. Meningioma with brain edema: Radiological characteristics on MRI and review of the literature. Clin. Imaging. 2002; 26(4): 243-9.
24. **Pott M, Huber M, Assheuer J, Bewermeyer H**. Comparison of MRI, CT and angiography in cerebral arteriovenous malformations. Bildgebung. 1992; 59(2):98-102.
25. **Mafee MF, James SG, James GG** Imaging of the chiasmal and juxtasellar regions. Ophthalmology Clinics of North America. 1996; 7(3): 347-66.
26. **Elster AD, Challa VR, Gilbert TH, Richardson DN, Contento JC**. Meningiomas: MR and histopathologic features. Radiology. 1989; 170(3 Pt 1):857-62.
27. **Young SC, Grossman RI, Goldberg HI, Spagnoli MV, Hackney DB, Zimmerman RA, et al**. MR of vascular encasement in parasellar masses: comparison with angiography and CT. American journal of neuroradiology. 1988; 9(1):35-8.
28. **Kasuya J, Hashimoto Y, Terasaki T, Miura M, Miyayama H, Uchino M.** Intracerebral hematoma in thalamus with incongruous right homonymous hemianopia: a case report. Rinsho Shinkeigaku. 2000; 40(1):29-33.

To Cite :

ALMALKI, Y. Evaluation of Anterior Visual Pathway Lesions Using CT and MRI: A Prospective Descriptive Study. *Zagazig University Medical Journal*, 2024; (264-275): -. doi: 10.21608/zumj.2021.99578.2369